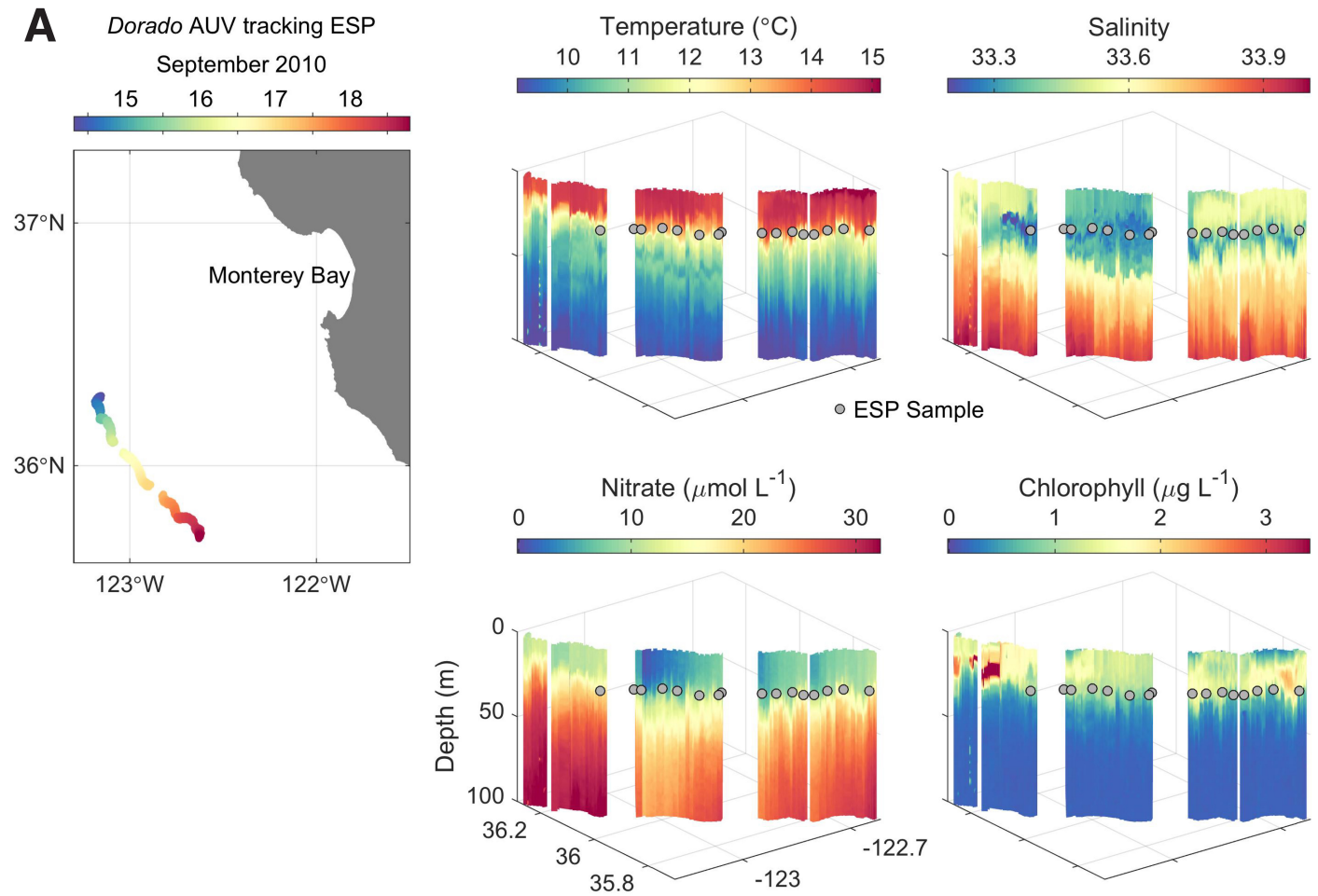


Supplementary File 2:

Supplementary Figures



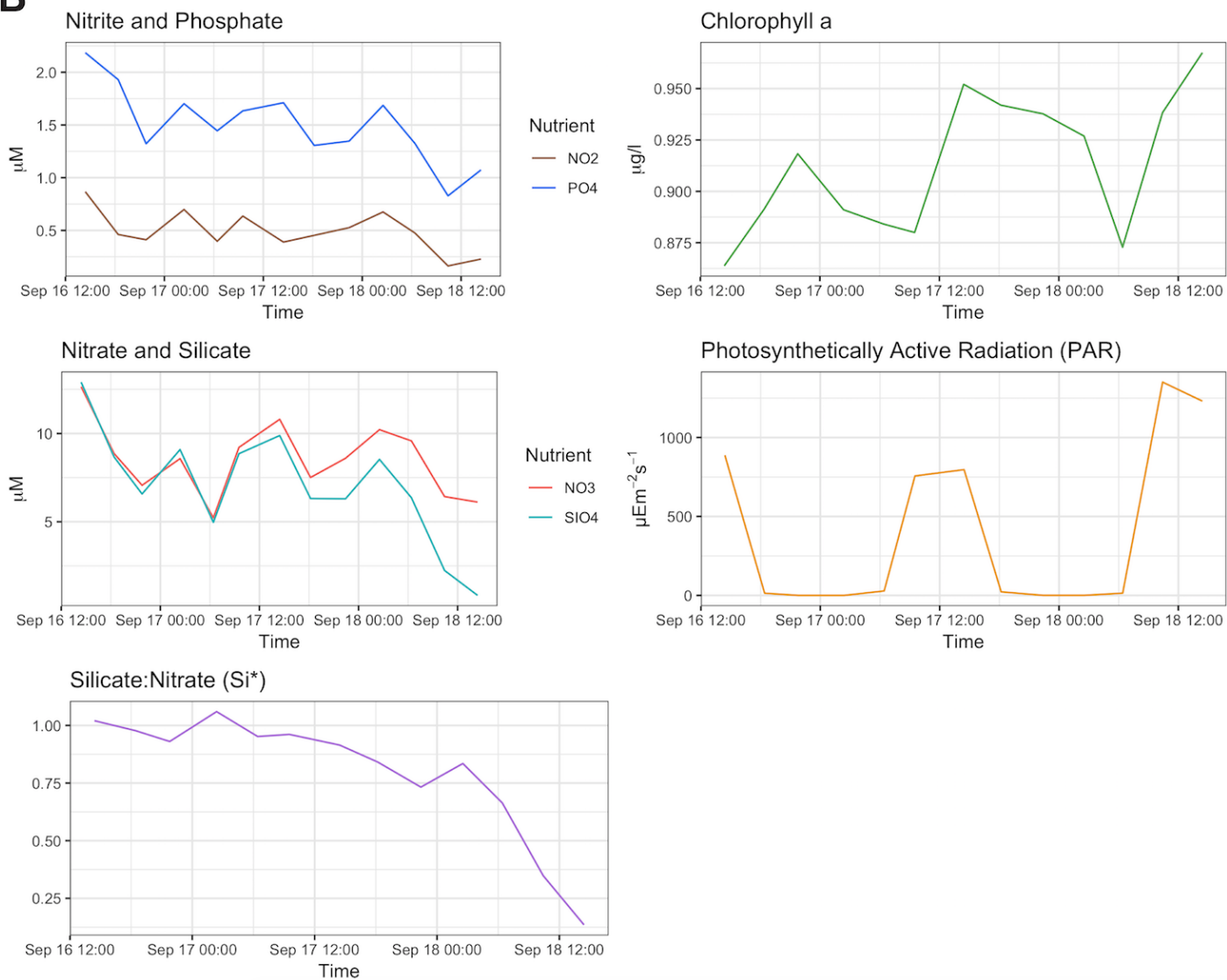
B

Figure S1 Biogeographical context of the drift track. **(A)** *In situ* oceanographic conditions of the drift track as observed by the *Dorado* AUV. Grey dots represent approximate locations of ESP samples. **(B)** Nutrients, chlorophyll, and light availability along the drift track at the depth of the ESP drift (~23m).

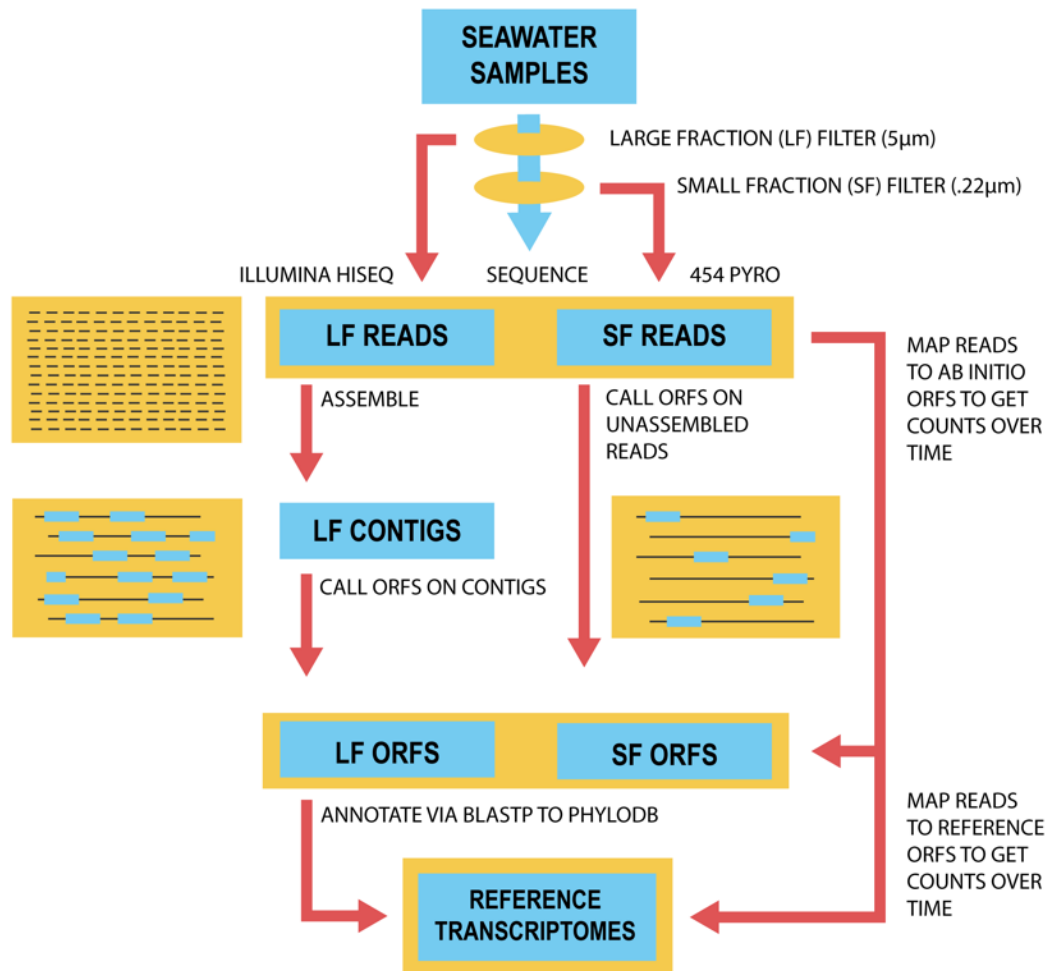


Figure S2 Bioinformatic pipeline. Seawater was collected onto 5µm and 0.22 µm filters, separating biomass into a large and small fraction, respectively. Large fraction (LF) reads were sequenced on the Illumina HiSeq platform, whereas small fraction (SF) reads had been previously sequenced by Ottesen *et al.* in 2012 on a GS FLX Titanium system (1). *Ab initio* ORF predictions were called on assembled large fraction contigs and directly on small fraction ORFs due to the longer read length, lower coverage nature of 454 sequencing. This less-restrictive amino acid space approach allowed us to map 7x more reads than traditional nucleotide space mapping to known references. Still, despite mapping 107 million reads, 158 million reads could not be mapped to *ab initio* ORFs, and those that did only averaged 67.2% identity to their best BLAST hit. Transcriptomes of reference organisms were chosen based on similarity and abundance of closely related species. Large and small fraction reads were mapped to reference transcriptomes using nucleotide Burrows Wheeler Aligner (BWA; (2)). Reference transcriptomes were hierarchically clustered together with large and small fraction ORFs to gene ortholog groups. The resultant clusters, reference transcriptomes, and de-novo ORFs from both fractions were annotated taxonomically and functionally and used for downstream analyses, including pattern recognition algorithms such as Harmonic Regression Analysis (HRA) and Weighted Gene Network Correlation Analysis (WGCNA).

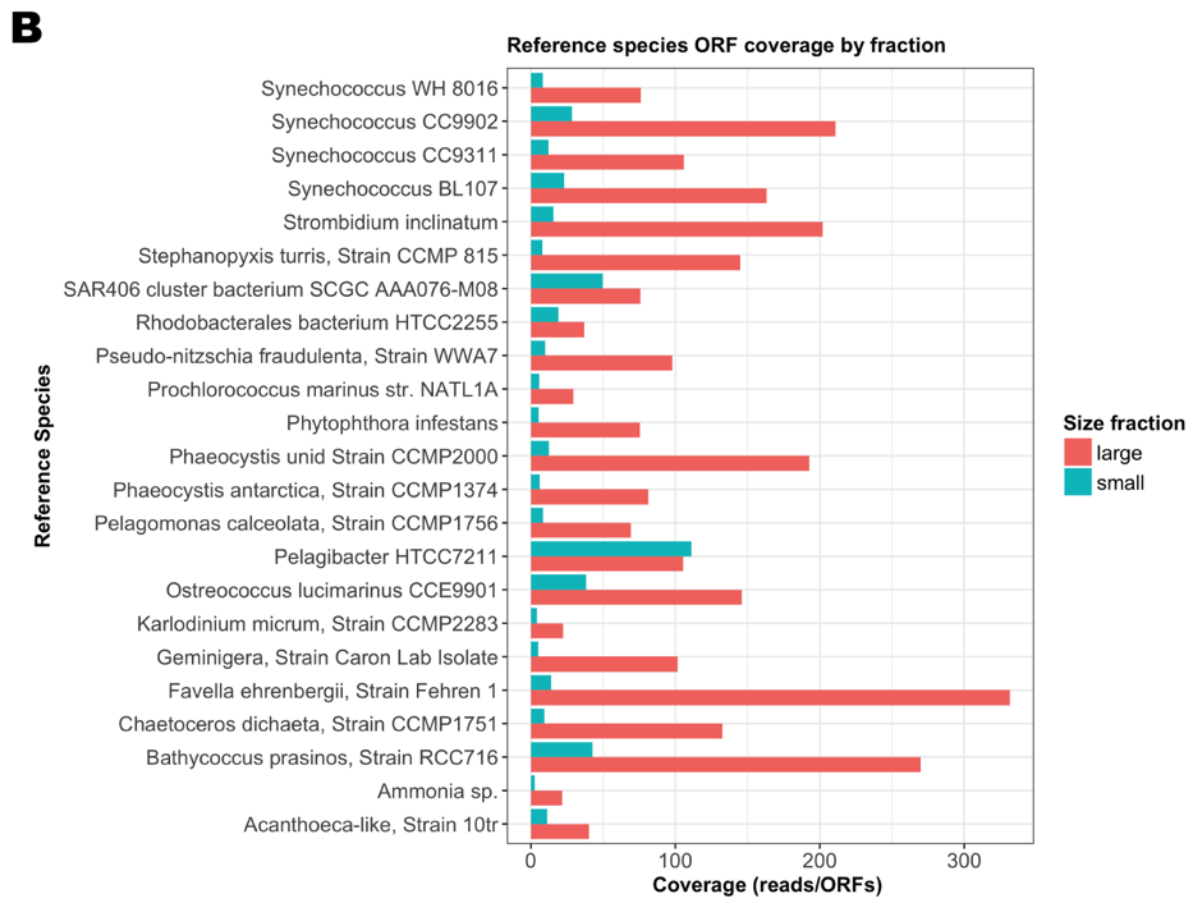
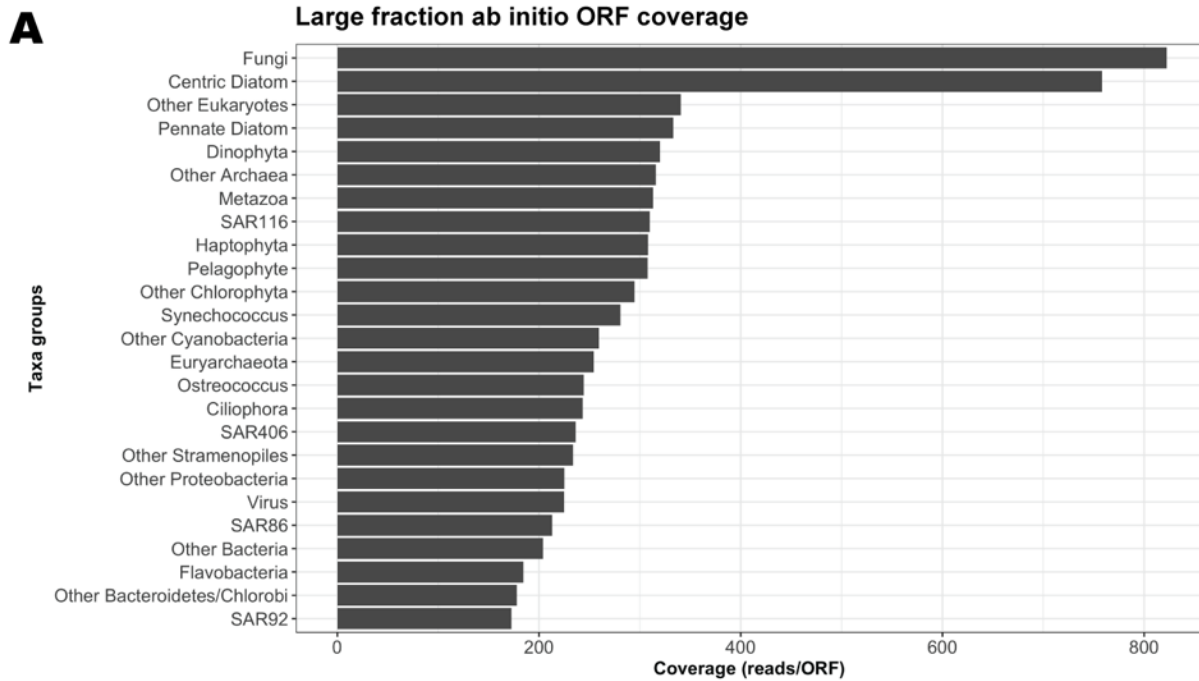


Figure S3 Depth of coverage of **(A)** large fraction *ab initio* ORFs by taxa group and **(B)** large and small fraction nucleotide references.

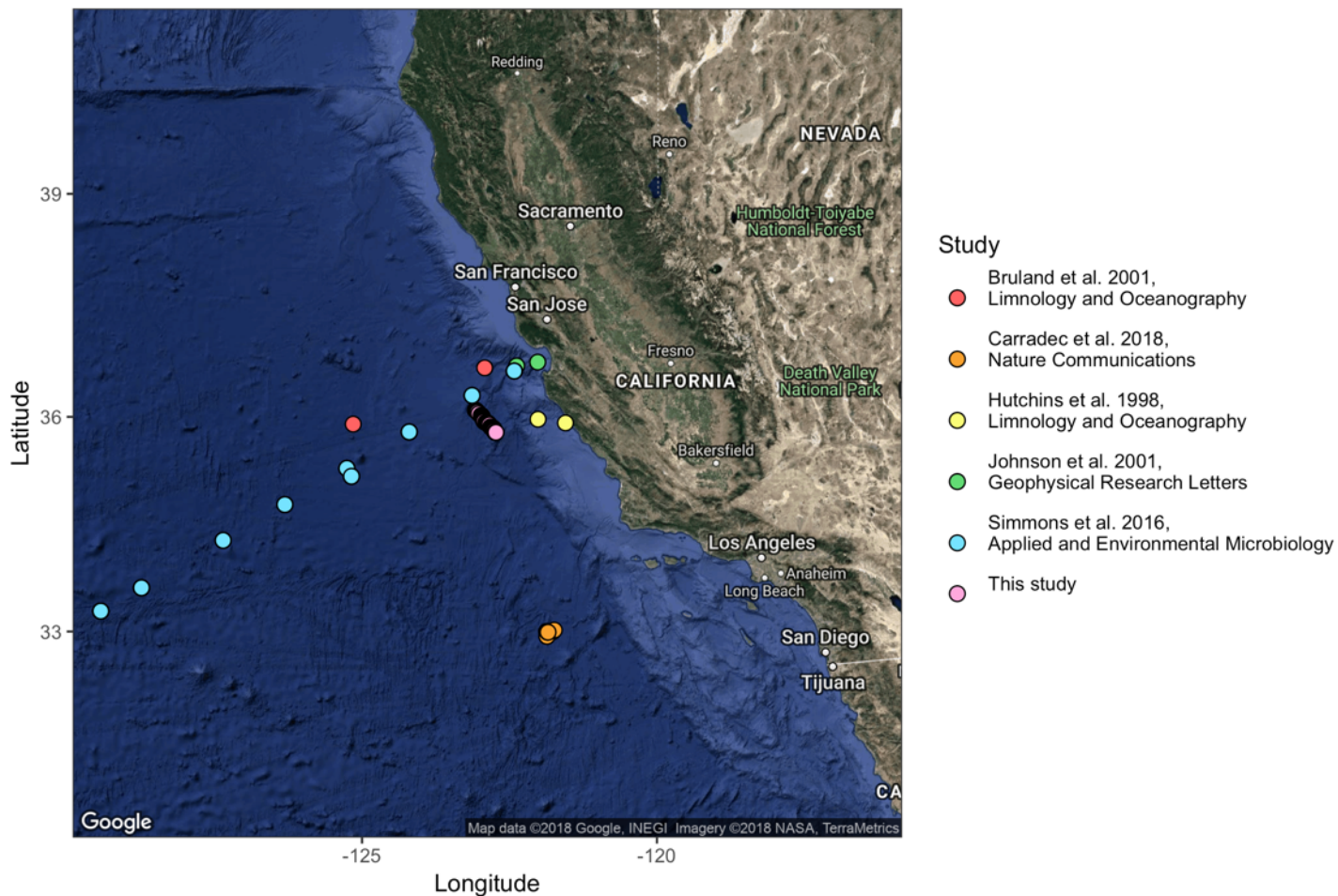


Figure S4 Location of drift track (pink) relative to sites with documented iron limitation (Supplementary Data 12E).

Red: July, 1995, measured total Fe < 0.05 nM, Fe-enrichment experiments confirm Fe limitation (3)

Orange: modeled total Fe < .04 umol/m³ based on global oceanographic data (4)

Yellow: June 1996/ June 1997, measured DPSCSV reactive Fe ≤ 0.1 nM, total Fe ≤ 0.1 nM, Fe-enrichment experiments confirm moderate to severe Fe limitation (5)

Green: Monterey Bay moorings M1 and M2, seasonal Fe limitation documented (e.g. June 1999/August 1999, measured total Fe < 1 nM) (6)

Blue: September-October 2009, total Fe < 1nM for at least 1 depth at given coordinates (7)

Figure S5 Expression of major nutrient cycling genes across size classes. Pies represent annotated functional clusters of *ab initio* ORFs and are colored by relative taxonomic contribution. The biogeochemical pathway each cluster participates in is noted in blue; asterisks denote ORFs previously observed to be transcriptionally sensitive to iron limitation. Clusters are grouped by modules of similar expression as given by WGCNA.

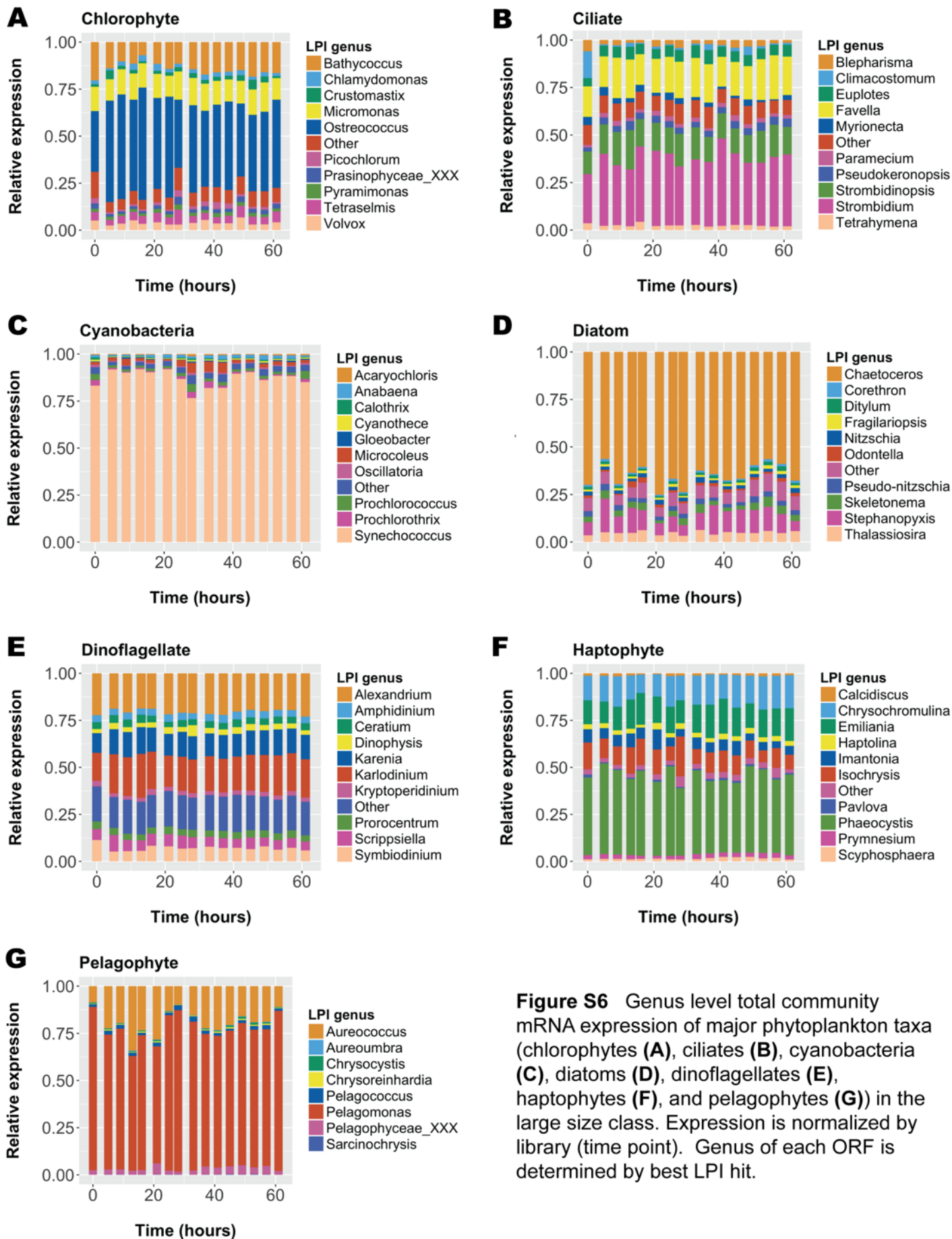


Figure S6 Genus level total community mRNA expression of major phytoplankton taxa (chlorophytes (A), ciliates (B), cyanobacteria (C), diatoms (D), dinoflagellates (E), haptophytes (F), and pelagophytes (G)) in the large size class. Expression is normalized by library (time point). Genus of each ORF is determined by best LPI hit.

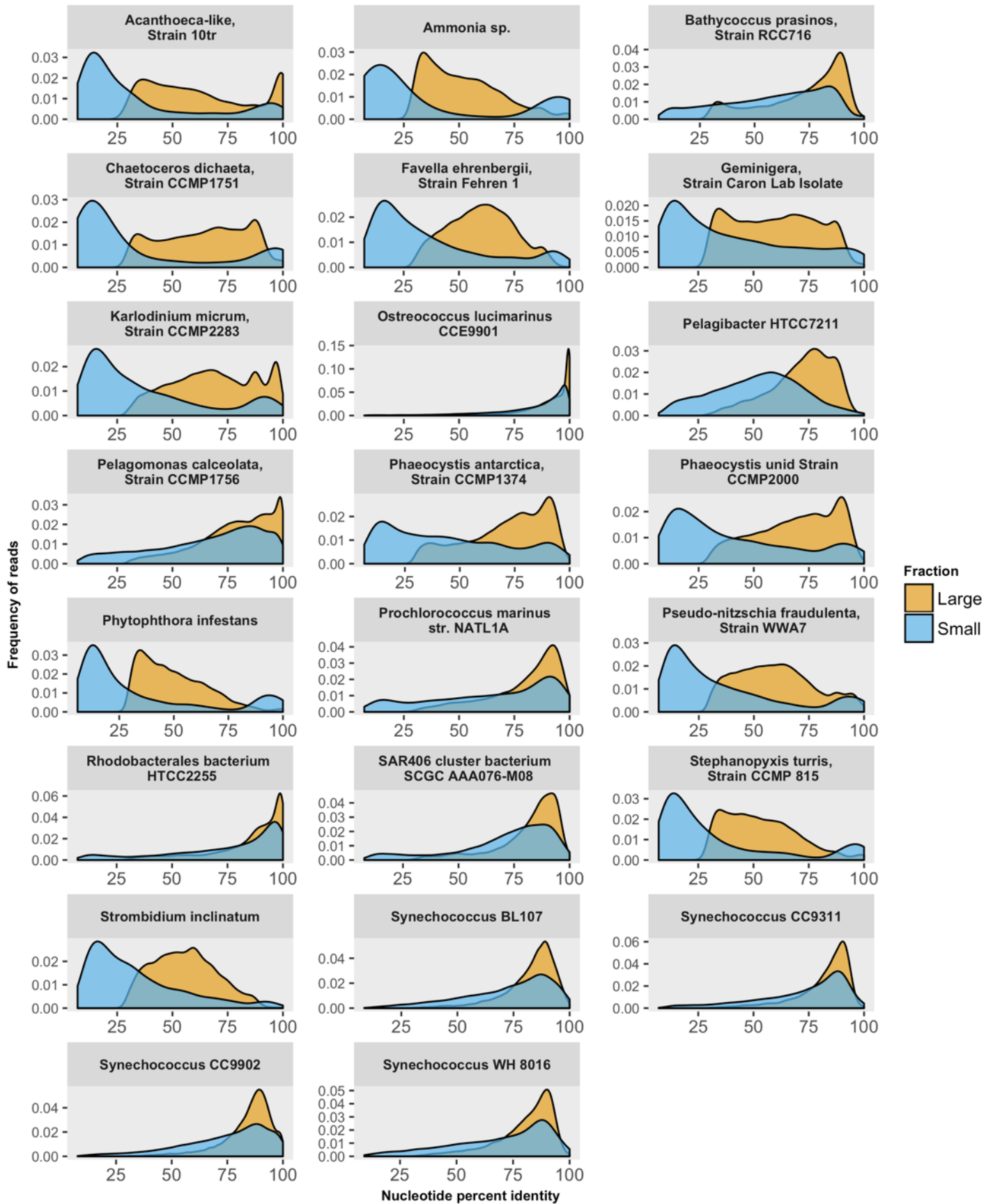


Figure S7 Average nucleotide percent identity of large fraction reads mapping to reference transcriptomes in the large (orange) and small (blue) size classes.

Percent identity of large fraction references

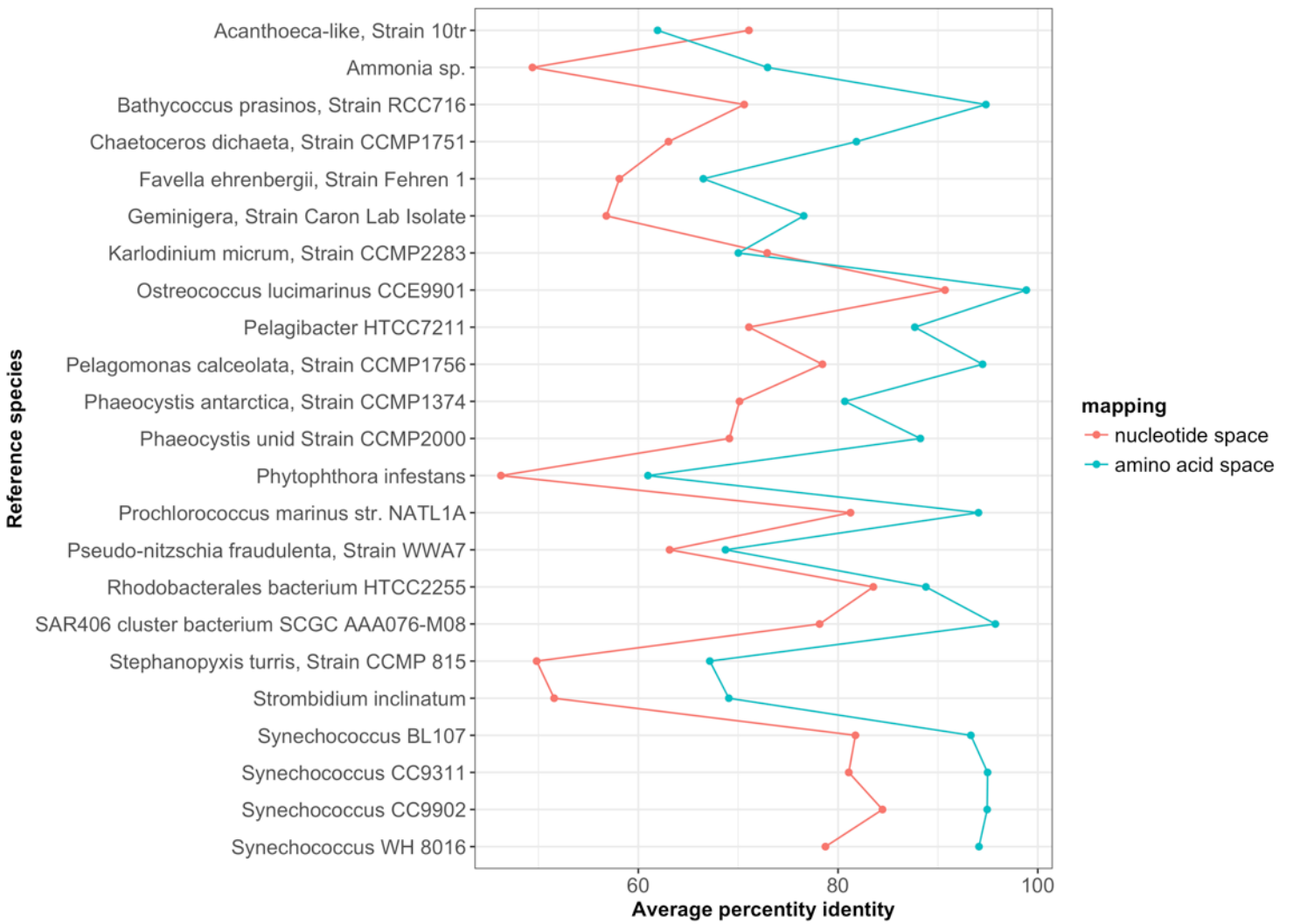


Figure S8 Comparison of average percent identity of reads mapping to reference transcriptomes in nucleotide space (red) and reads mapping to *ab initio* ORFs in amino acid space (blue).

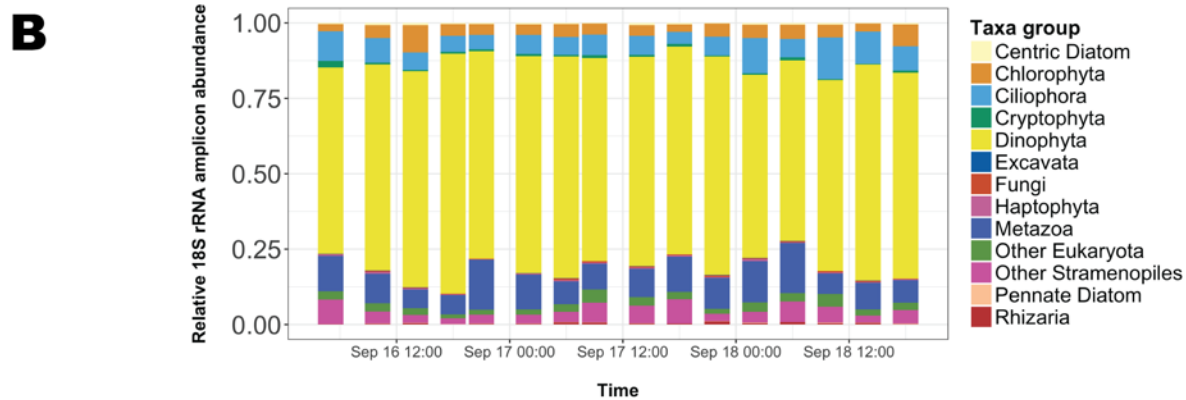
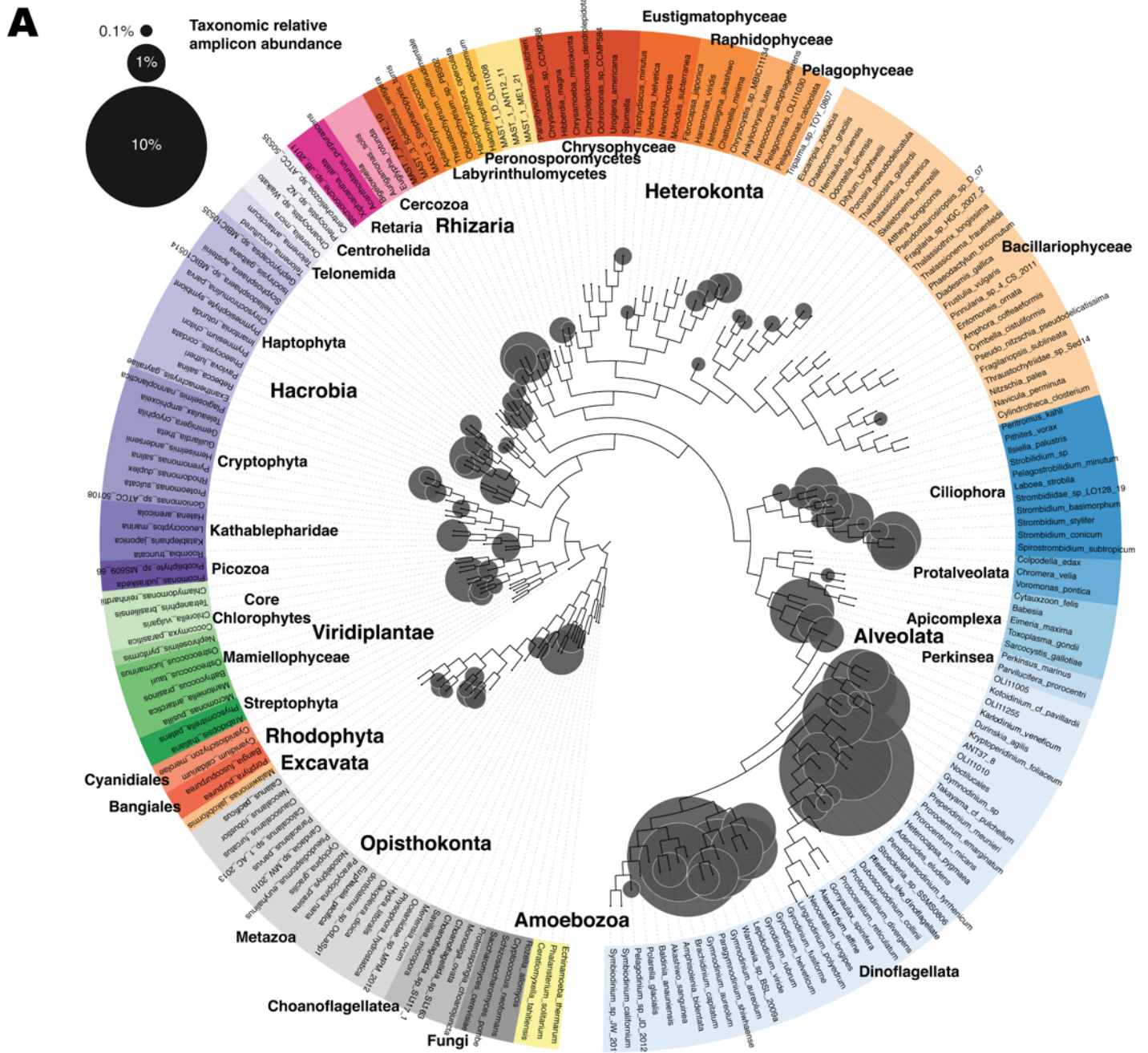


Figure S9 (A) Phylogenetic tree showing distribution of active large fraction eukaryotes using 18S rRNA amplicons (Supplementary Data 3). Circles representing relative amplicon abundance are superimposed over a reference phylogeny which is colored by taxonomy. Proximity of circles to the

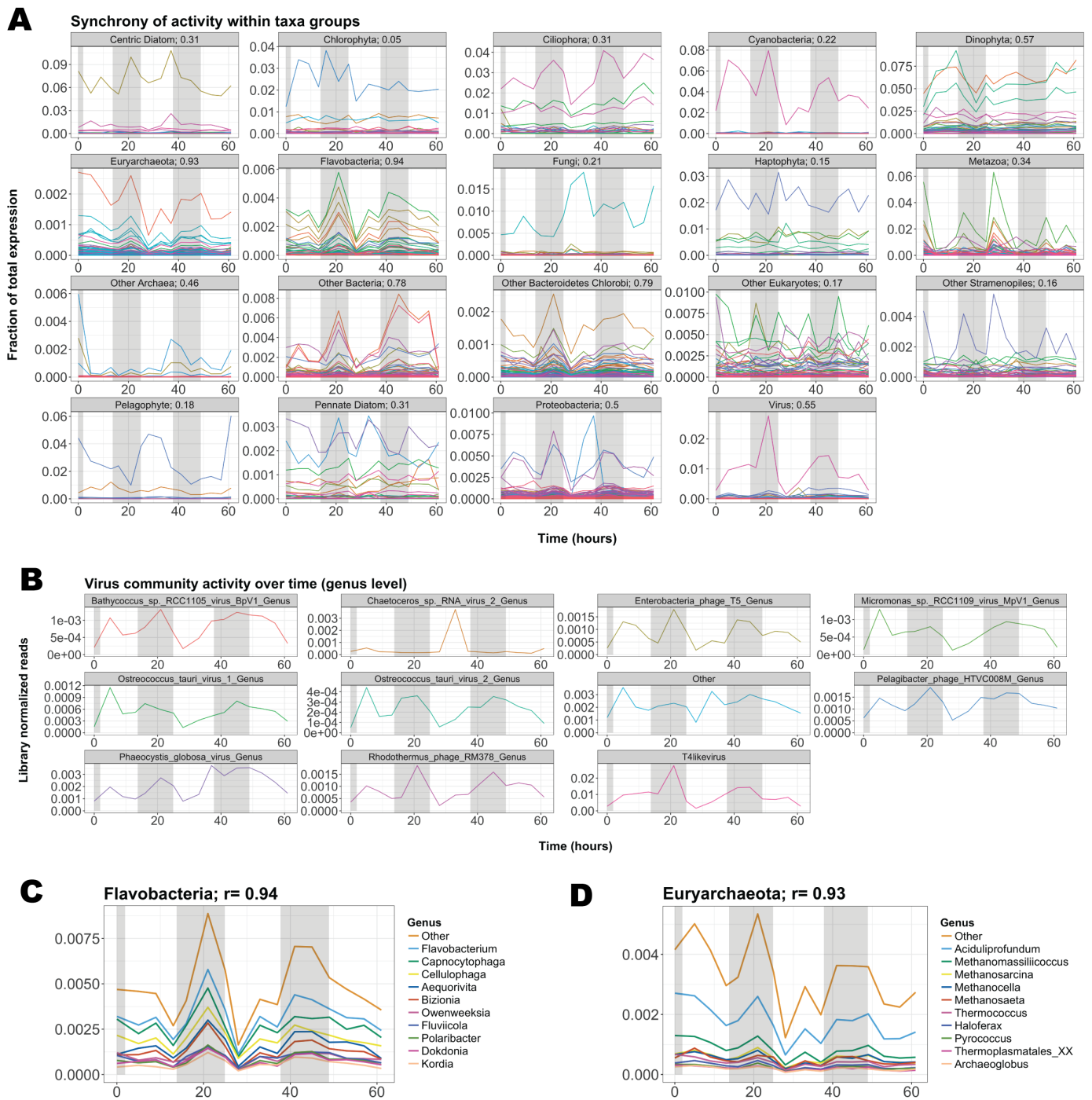


Figure S11 Synchronization of total activity among related organisms in the large fraction as viewed using *ab initio* ORFs. **(A)** Library (time point) normalized expression of *ab initio* ORFs binned by LPI-based taxonomic group. Numbers in headers denote strength of correlation between ORFs in a shared taxa group (Pearson's r). **(B)** Library normalized expression of top 10 large fraction virus genera. **(C)** and **(D)** show genus-level contributions of highly synchronous *Flavobacteria* and *Euryarchaeota* groups, respectively.

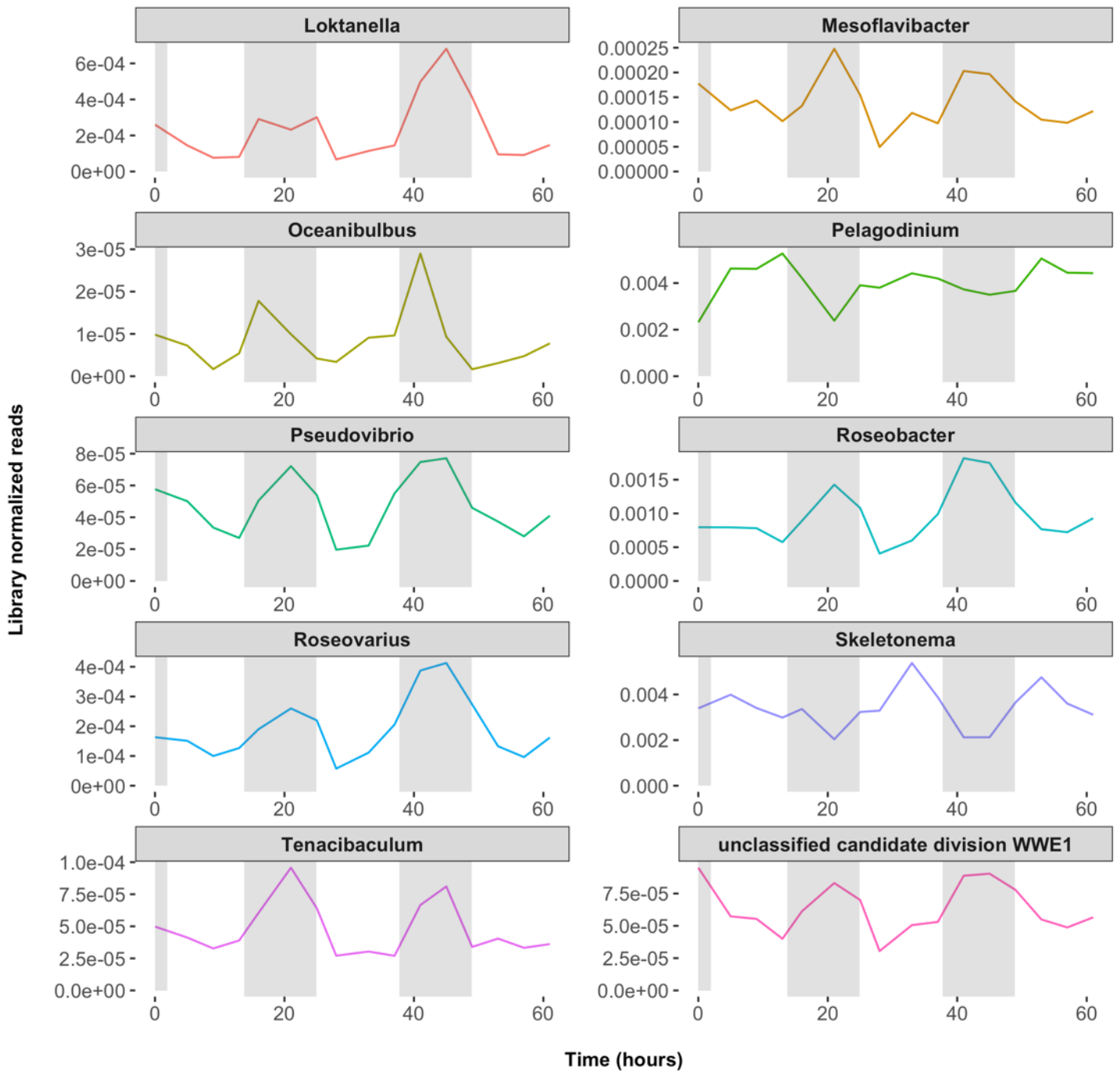
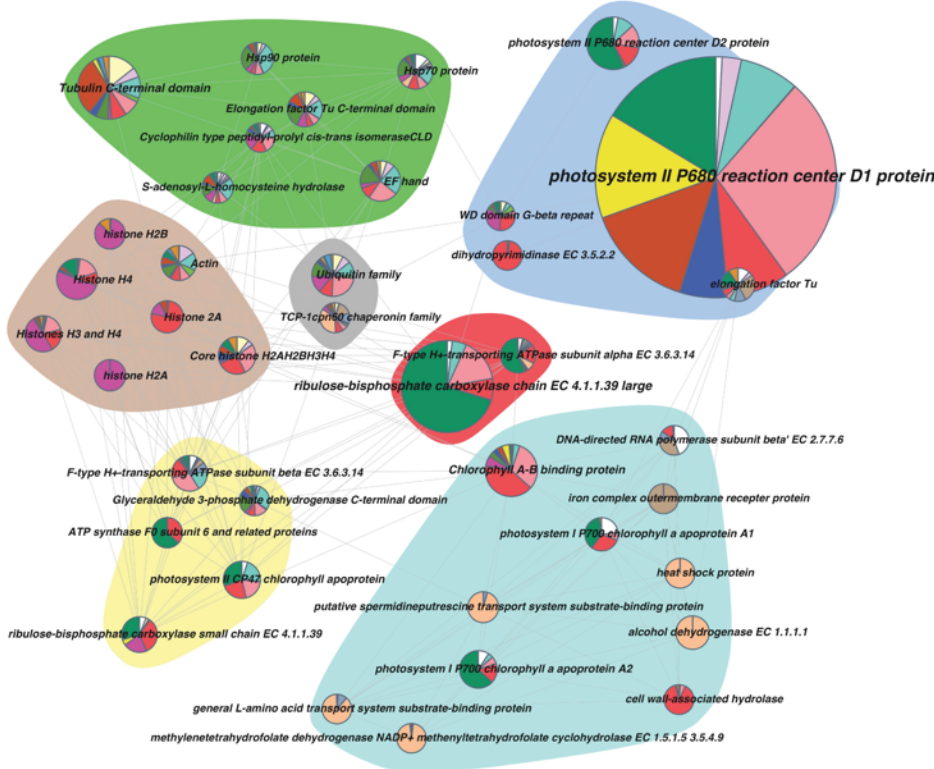
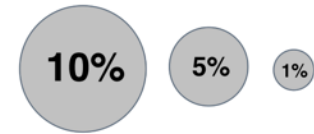


Figure S12 Total library (time point) normalized activity of large fraction genera that exhibit significant 24-h periodicity (HRA; FDR $p \leq 0.1$). Two photosynthetic eukaryotes, *Pelagodinium*, a photosynthetic dinoflagellate symbiotic with foraminifera (8), and the centric diatom *Skeletonema*, had peak activity during the day. The remaining genera were non-photosynthetic bacteria with aggregate gene expression peaking at night: *Loktanella*, *Mesoflavibacter*, *Oceanibulbus*, *Pseudovibrio*, *Roseobacter*, *Roseovarius*, *Tenacibaculum*, and *Unclassified candidate division WWE1*. Several are known phytoplankton associates (e.g. *Loktanella* spp. (9,10)) and early particle colonizers (11) not previously known to operate on a diel cycle.

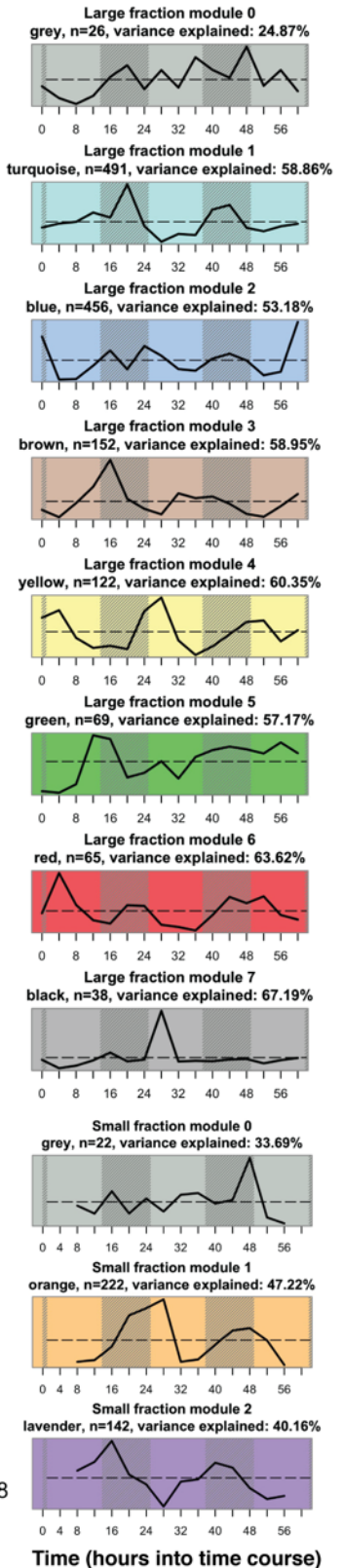
Large fraction (> 5µm) functional clusters



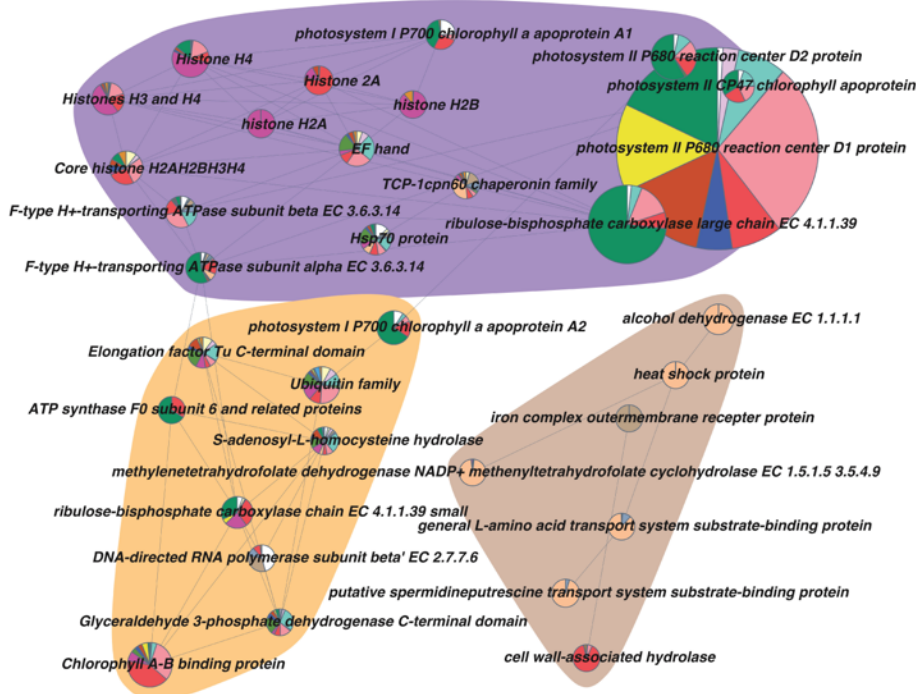
Cluster expression scale (Percent of size class mapped reads)



Expression modules



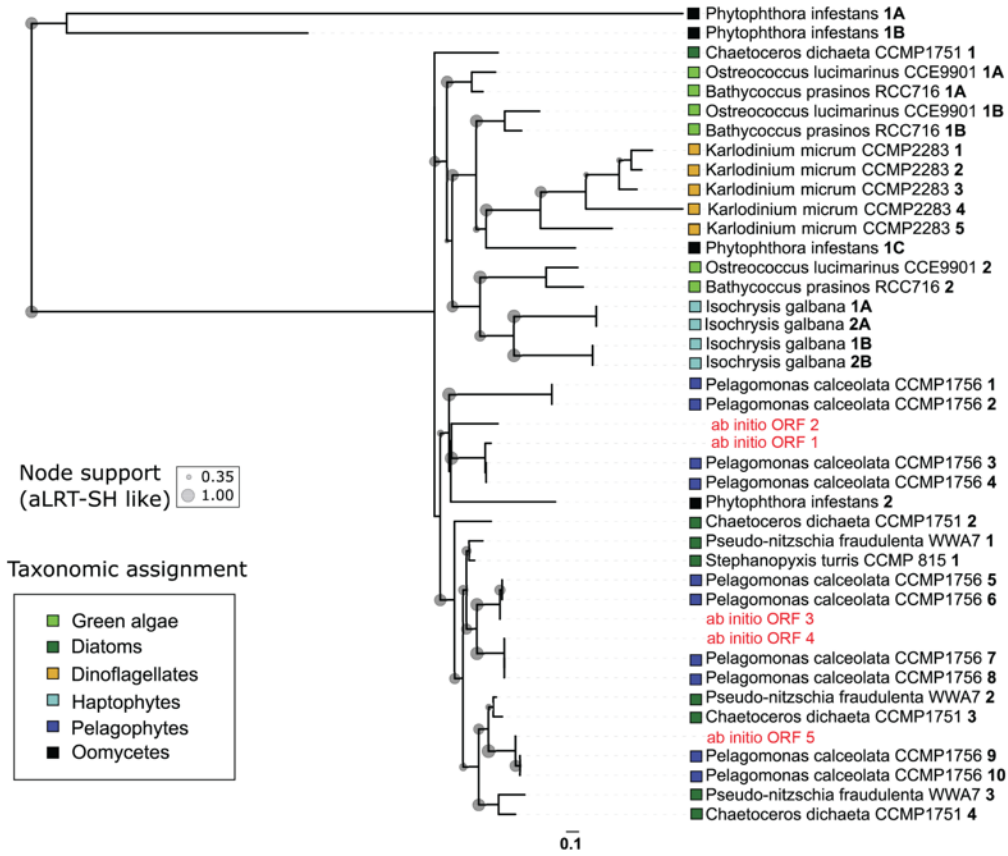
Small fraction (> .22µm) functional clusters



Reference species

- Acanthoeca like Strain 10tr
- Ammonia sp
- Bathycoccus prasinos Strain RCC716
- Chaetoceros dicaeta Strain CCMP1751
- Favella ehrenbergii Strain Fehren 1
- Geminigera Strain Caron Lab Isolate
- Karlodinium micrum Strain CCMP2283
- Ostreococcus lucimarinus CCE9901
- Pelagibacter HTCC7211
- Pelagomonas calceolata Strain CCMP1756
- Phaeocystis spp
- Phytophthora infestans
- Prochlorococcus marinus str NATL1A
- Pseudo nitzschia fraudulenta Strain WWA7
- Rhodobacterales bacterium HTCC2255
- SAR406 cluster bacterium SCGC AAA076 M08
- Stephanopyxis turris Strain CCMP 815
- Strombidium inclinatum
- Synechococcus spp

Figure S13 A comparison of functional diversity across fractions by mapping reads to transcriptomes of cultured representatives. Pies represent most abundant functional clusters of reference ORFs. Pies are colored by relative taxonomic contribution and grouped by modules of similar expression as given by WGCNA. Note that reads mapping to *Favella ehrengbergii* Strain Fehren 1 (e.g. those involved in photosynthesis) may be hitting remnants of its photosynthetic food source.

A**B**

C	Transcript ID	Pfam domain ID	Domain description	Corresponding genus & species IDs on the LOV tree
Reference transcripts	CAMPEP_0199691428-CAMNT_0045556983	PF07716, PF13426	bZIP_2 (basic leucine zipper), PAS_9	Pelagomonas calceolata CCMP1756 6
	CAMPEP_0199699820-CAMNT_0045565857	PF13426	PAS_9	Pelagomonas calceolata CCMP1756 4
	CAMPEP_0199705234-CAMNT_0045571731	PF07716, PF13426	bZIP_2 (basic leucine zipper), PAS_9	Pelagomonas calceolata CCMP1756 10
	CAMPEP_0199709614-CAMNT_0045576641	PF07716, PF13426	bZIP_2 (basic leucine zipper), PAS_9	Pelagomonas calceolata CCMP1756 8
	CAMPEP_0199710938-CAMNT_0045577979	PF13426	PAS_9	Pelagomonas calceolata CCMP1756 2
	contig_10685_301_1296-Pelagomonas	PF13426	PAS_9	Pelagomonas calceolata CCMP1756 3
	contig_12486_283_1311-Pelagomonas	PF07716, PF13426	bZIP_2 (basic leucine zipper)	Pelagomonas calceolata CCMP1756 7
	contig_40022_3223_3810-Pelagomonas	PF13426	PAS_9	Pelagomonas calceolata CCMP1756 9
	contig_5472_151_1554-Pelagomonas	PF13426	PAS_9	Pelagomonas calceolata CCMP1756 1
	contig_8318_666_1631-Pelagomonas	PF07716, PF13426	bZIP_2 (basic leucine zipper), PAS_9	Pelagomonas calceolata CCMP1756 5
	GGTG_05190T0-supercont13	PF13426, PF08447, PF00320	PAS_9, PAS_3, GATA (GATA zinc finger domain)	Phytophthora infestans 1A, 1B, 1C
	GGTG_12596T0-supercont19	PF13426	PAS_9	Phytophthora infestans 2
	Karlodinium-micrum-CCMP2283-20140214 17716_1	PF13426	PAS_9	Karlodinium micrum, Strain CCMP2283 3
	Karlodinium-micrum-CCMP2283-20140214 19826_1	PF13426, PF00069	PAS_9, Protein kinase domain	Karlodinium micrum, Strain CCMP2283 4
	Karlodinium-micrum-CCMP2283-20140214 23659_1	PF13426	PAS_9	Karlodinium micrum, Strain CCMP2283 2
	Karlodinium-micrum-CCMP2283-20140214 29782_1	PF00069, PF13426	Protein kinase domain, PAS_9	Karlodinium micrum, Strain CCMP2283 5
	Karlodinium-micrum-CCMP2283-20140214 4888_1	PF13426	PAS_9	Karlodinium micrum, Strain CCMP2283 1
	MMETSP0123-20130129 11670_1	PF13426	PAS_9	Isochrysis galbana 2A, 2B
	MMETSP0123-20130129 18638_1	PF13426	PAS_9	Isochrysis galbana 1A, 1B
	MMETSP0794_2-20130614 17546_1	PF07716, PF13426	bZIP_2 (basic leucine zipper), PAS_9	Stephanopyxis turris CCMP 815 1
	MMETSP1447-20131203 31680_1	PF00170, PF13426	Basic leucine zipper (bZIP_1), PAS_9	Chaetoceros dictyota CCMP1751 3
	MMETSP1447-20131203 5598_1	PF13426	PAS_9	Chaetoceros dictyota CCMP1751 1
	MMETSP1447-20131203 66049_1	PF07716, PF13426	bZIP_2 (basic leucine zipper), PAS_9	Chaetoceros dictyota CCMP1751 4
	MMETSP1447-20131203 9341_1	PF07716, PF13426	bZIP_2 (basic leucine zipper), PAS_9	Chaetoceros dictyota CCMP1751 2
	MMETSP1460-20131121 1537_1	PF13426, PF00069	PAS_9, Protein kinase domain	Bathycoccus prasinos RCC716 1A, 1B
	MMETSP1460-20131121 31452_1	PF13426, PF00512, PF02518, PF00072	PAS_9, HisKA (Histidine kinase), GHKL (Gyrase-Hsp90-Histidine Kinase-MutL), Response regulator receiver domain	Bathycoccus prasinos, Strain RCC716 2
	OSTLU_35077-NC_009363	PF13426	PAS_9	Ostreococcus lucimarinus CCE9901 2
	OSTLU_40751-NC_009369	PF13426, PF00069	PAS_9, Protein kinase domain	Ostreococcus lucimarinus CCE9901 1A & 1E
	Pseudo_nitzschia-fraudulenta-WWA7-20140214 1617_1	PF00170, PF13426	Basic leucine zipper (bZIP_1), PAS_9	Pseudo-nitzschia fraudulenta WWA7 3
	Pseudo_nitzschia-fraudulenta-WWA7-20140214 45782_1	PF00170, PF13426	Basic leucine zipper (bZIP_1), PAS_9	Pseudo-nitzschia fraudulenta WWA7 2
	Pseudo_nitzschia-fraudulenta-WWA7-20140214 86850_1	PF00170, PF13426	Basic leucine zipper (bZIP_1), PAS_9	Pseudo-nitzschia fraudulenta WWA7 1
<i>ab initio</i> ORFs	contig_318056_1_312_+	PF13426	PAS_9	<i>ab initio</i> ORF 1
	contig_595760_1_551_-	PF13426	PAS_9	<i>ab initio</i> ORF 2
	contig_608828_30_709_-	PF07716, PF13426	bZIP_2 (basic leucine zipper), PAS_9	<i>ab initio</i> ORF 3
	contig_620084_102_530_+	PF13426	PAS_9	<i>ab initio</i> ORF 4
	contig_492140_1_541_-	PF13426	PAS_9	<i>ab initio</i> ORF 5

Figure S14 (A) Maximum likelihood phylogenetic tree of the LOV domains from select *ab initio* ORFs and reference transcripts. Branch labels indicate the species of origin of the reference transcripts (in black). “*ab initio*” prefix refers to transcripts assembled directly from the metatranscriptomic datasets (in red). Numeric suffixes added to the labels (in bold letters) indicate the number of LOV domain transcripts present in each species. Several transcripts harbor multiple LOV domains which are denoted by an additional suffix (A, B, C). For example, one transcript from *Phytophthora infestans* harbors three LOV domains and all of these are shown on the tree. Colored squares denote the taxonomic affiliations of the reference transcripts. **(B)** Expression profile of the reference transcripts and *ab initio* ORFs along the sampling period as Z-scores. Night and day periods are denoted by dark and light bars above the heatmap. **(C)** Table indicating the transcript ID, Pfam annotation, and corresponding taxonomic information for LOV domain containing reference and *ab initio* ORFs. Several lineages of eukaryotic phytoplankton showed ORFs possessing LOV (Light-Oxygen-Voltage) domains with peak activity just before dawn. LOV domains respond to blue light (12) and well-characterized LOV domain containing proteins are known to convert photosensory stimuli into downstream biochemical signal (13) via adjacent effector domains like serine-threonine kinases (in case of phototropins) or basic leucine zipper (b-ZIP) transcription regulatory domains (in case of Aureochromes) (14). In addition, a large number of novel LOV- effector domain combinations have been previously identified across the tree of life (15). Consistent with previous observations, we found aureochrome-like domain combinations in pelagophytes (16) and diatoms (17) and a phototropin like domain combination (LOV-protein kinase) in *Ostreococcus* (18) and *Bathycoccus*. Although presence and possible function of LOV domain containing proteins have not been discussed in dinoflagellates or oomycetes, we detected LOV-protein kinase domain combinations in *Karlodinium* and a GATA zinc finger – LOV combination in oomycetes *Phytophthora*. However, the expressions of these proteins were very low and did not follow a clear diel pattern. A vast majority of the reference and *ab initio* transcripts had peak expression at dawn, irrespective of the domain combinations, indicating a common light-regulated signaling/transcriptional response mediated by the LOV domain in these organisms.

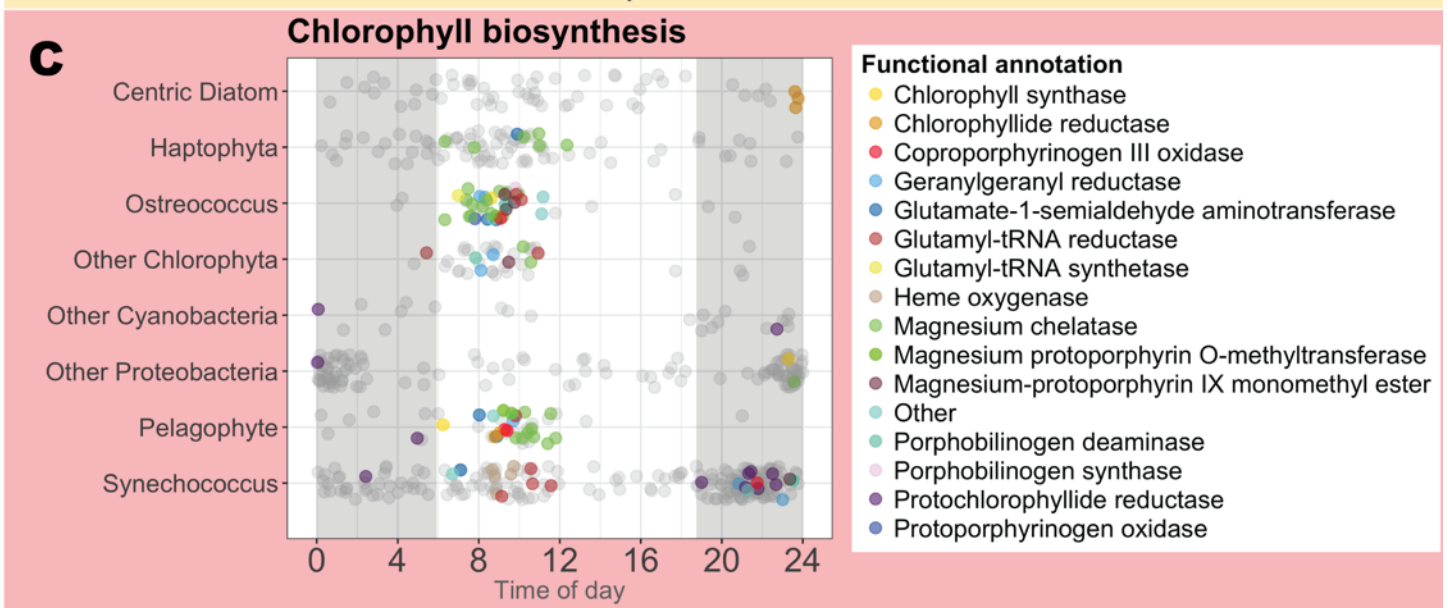
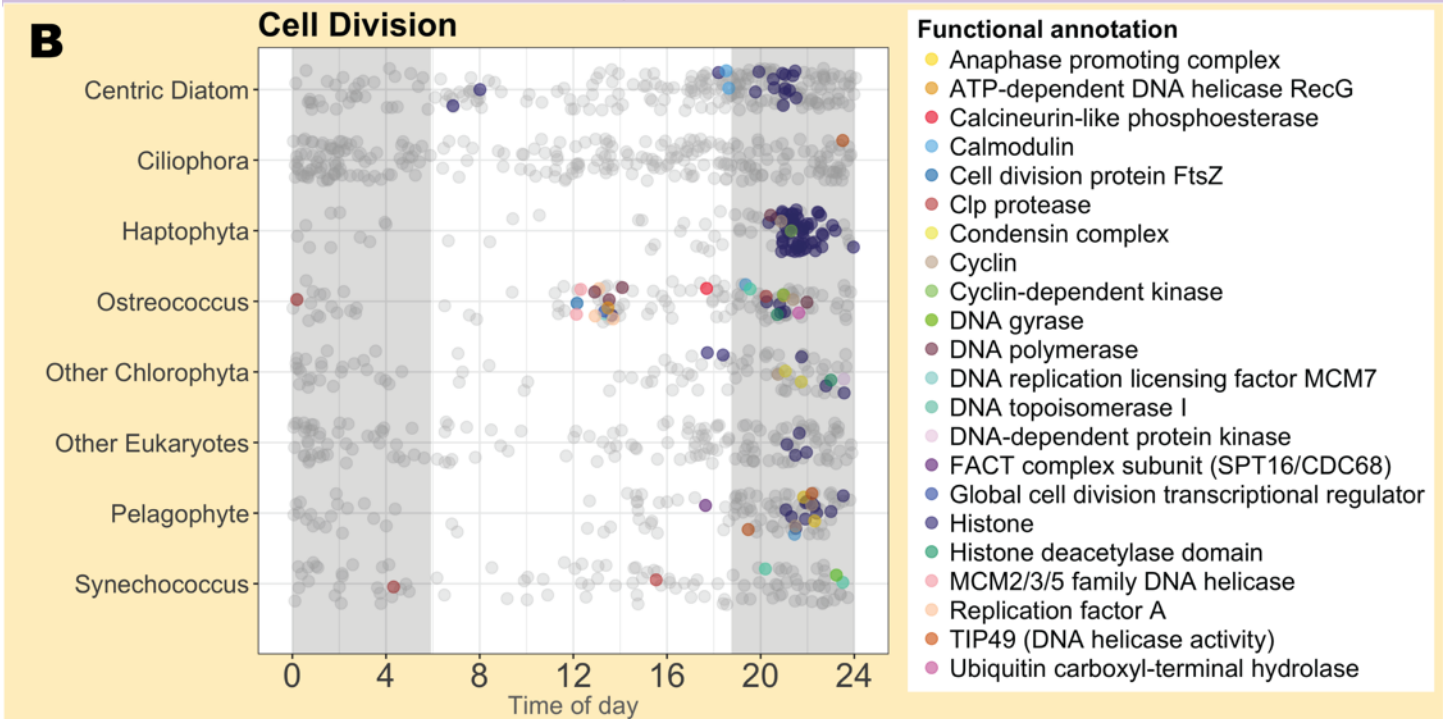
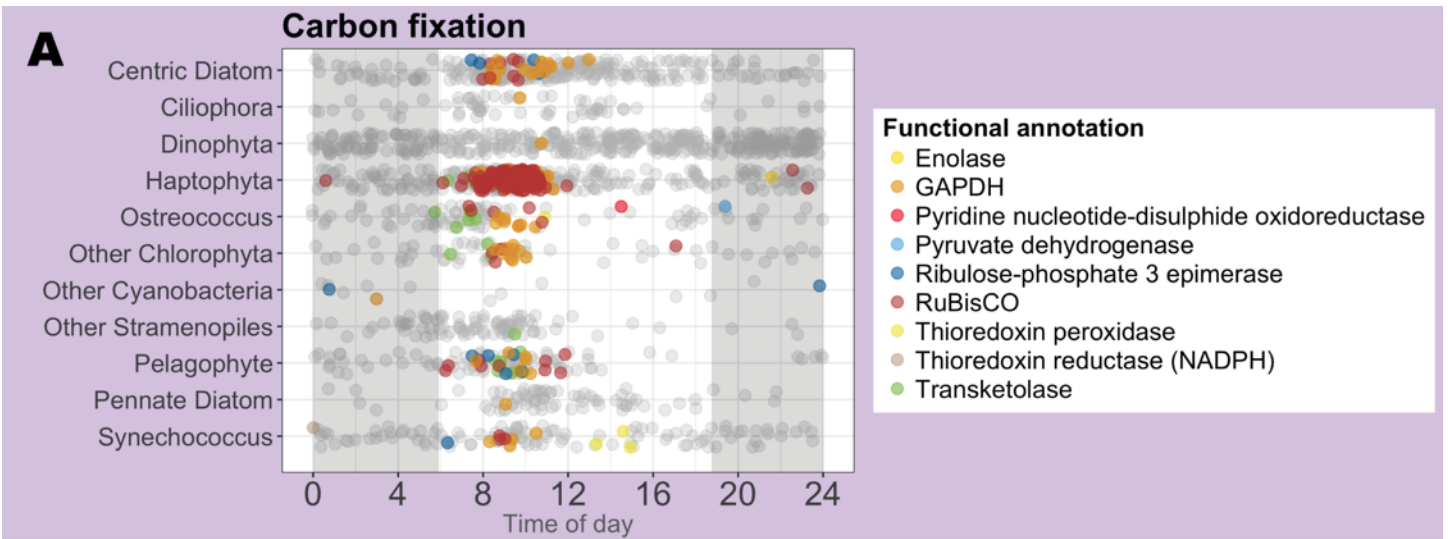


Figure S15 Peak expression time of large fraction ORFs involved in **(A)** carbon fixation, **(B)** cell division, and **(C)** chlorophyll biosynthesis. Night is indicated by grey shading, while white represents daylight hours. Significantly periodic ORFs (HRA; FDR adjusted $p \leq 0.1$) are colored by functional annotation; insignificant ORFs are shown in grey.

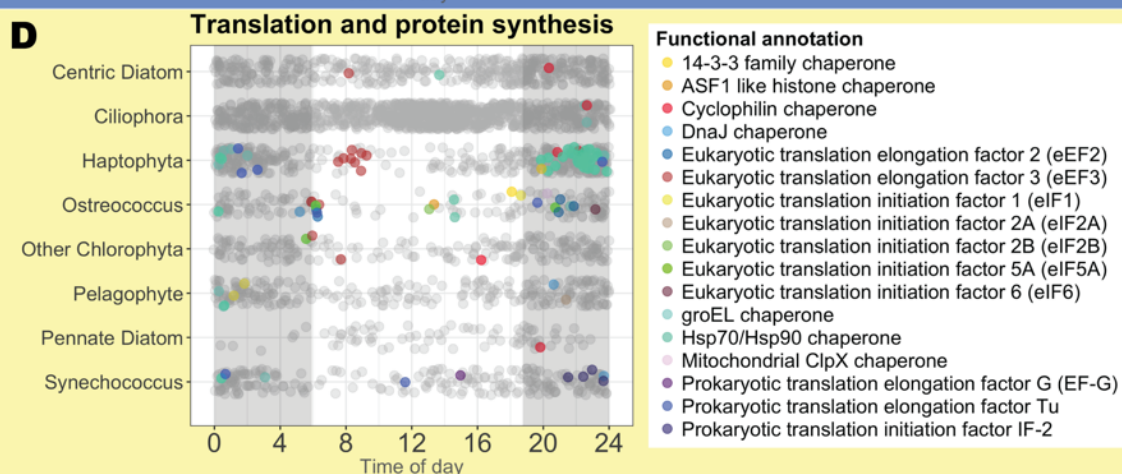
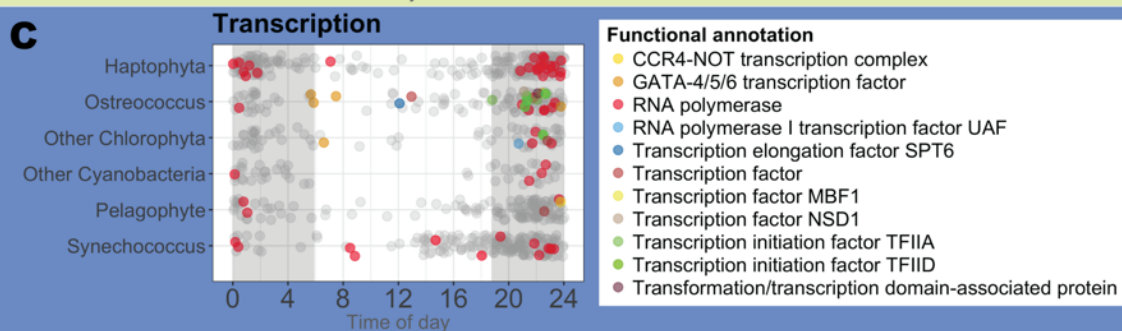
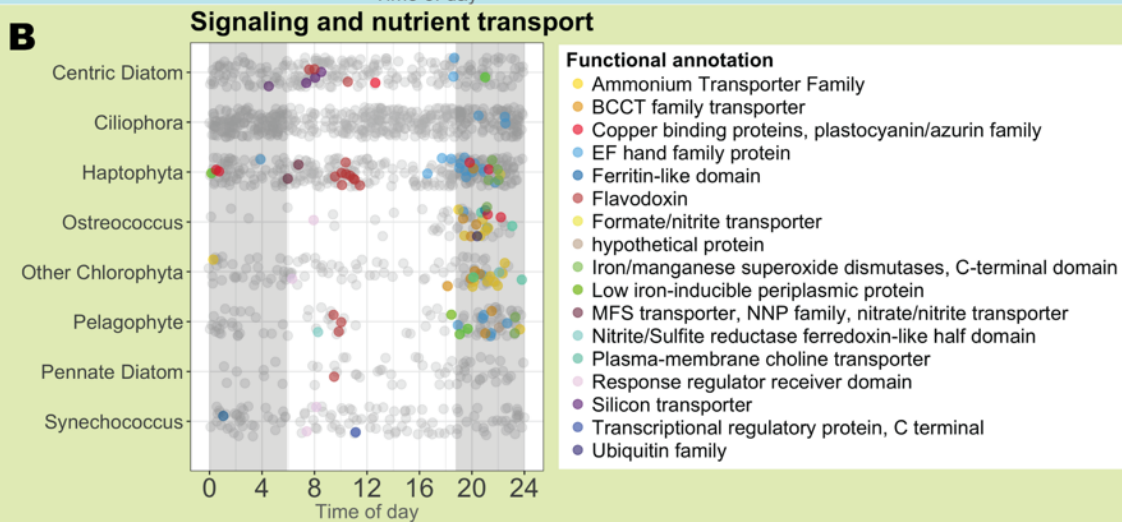
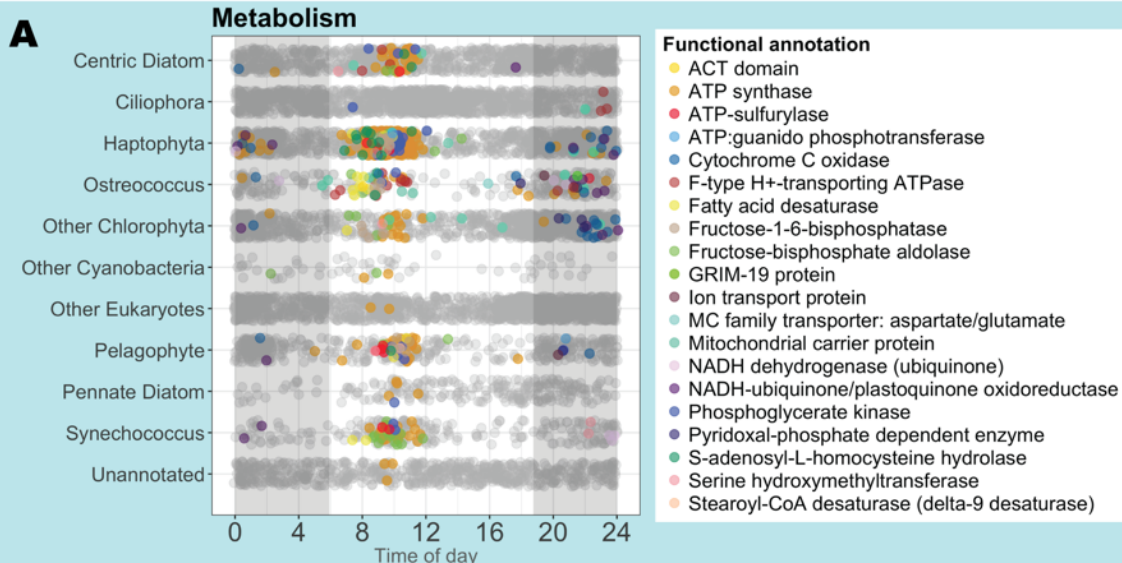


Figure S16 Peak expression time of large fraction ORFs involved in **(A)** metabolism, **(B)** signaling and nutrient transport, **(C)** transcription and **(D)** translation and protein synthesis. Night is indicated by grey shading. Significantly periodic ORFs (HRA; FDR adjusted $p \leq 0.1$) are colored by functional annotation; insignificant ORFs are shown in grey. Several eukaryotic translation elongation factor 3 (eEF3) *ab initio* ORFs detected in the large size class were significantly periodic (dark red). eEF3 presents a novel peptide synthesis mechanism for phytoplankton. eEF3 was previously thought to be unique to fungi, but homologs have been recently discovered in various phytoplankton lineages, and one haptophyte (*Phytophthora infestans*) eEF3 was proven capable of restoring function in yeast (19). Of the 122 eEF3 ORFs in our data, the majority belonged to dinoflagellates, but several were also found among haptophytes (9 ORFs), chlorophytes (9), centric (7) and pennate (3) diatoms, pelagophytes (4), other stramenopiles (1) and even ciliates (1).

Peak time of day of periodic photosynthesis ORFs across ESP drifts

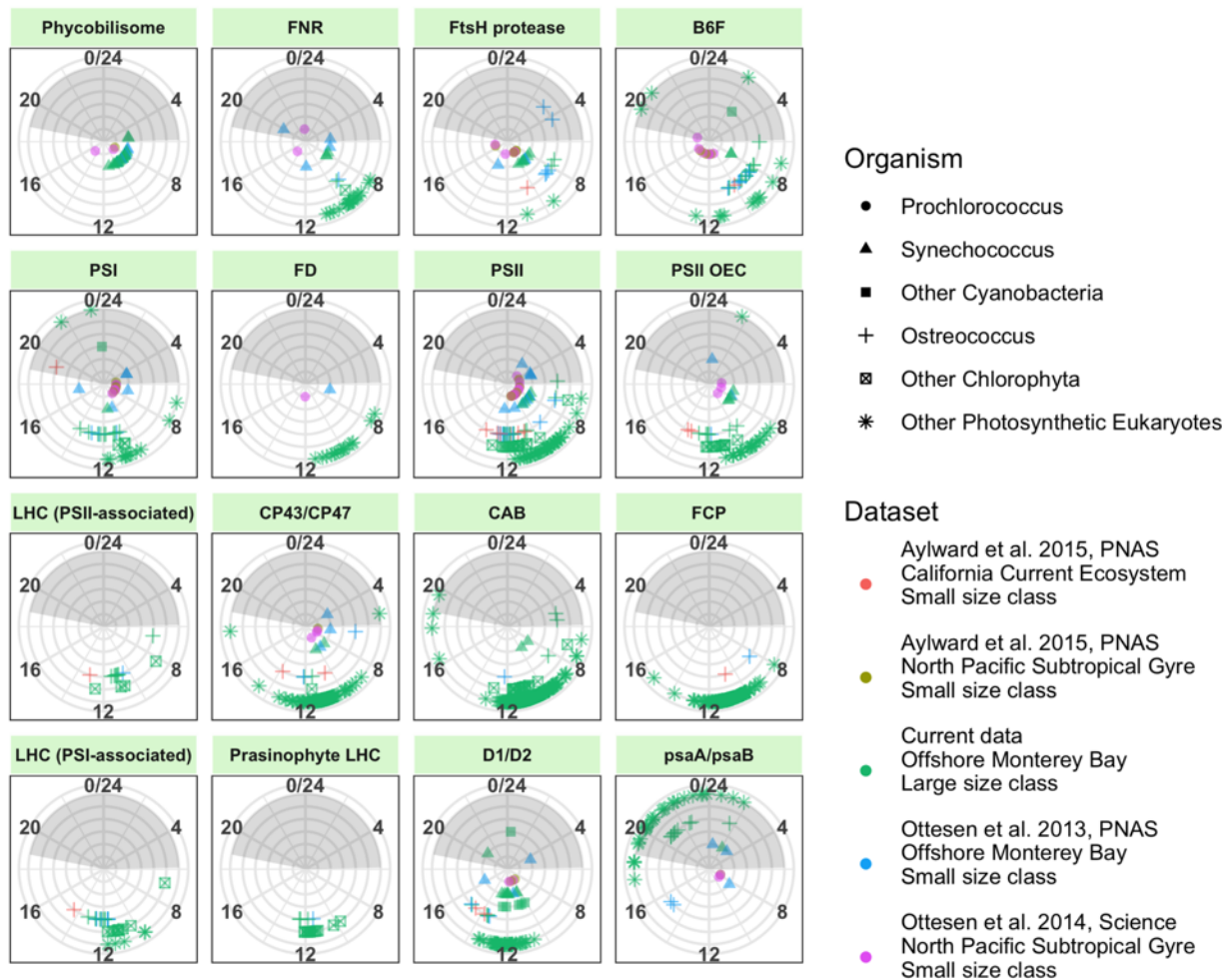



Figure S17 Comparison of peak expression time of photosynthesis related ORFs between the current data and previously studied ESP drift tracks (1,20,21). Taxa groups are distinguished by shape (legend, top right) and radius (innermost: *Prochlorococcus*, outermost: “Other Photosynthetic Eukaryotes”). Colors indicate dataset of origin. Night (as observed for current data) is indicated by grey shading. In some cases, addition of picoplankton data from other environments revealed a difference in timing between prokaryotic and eukaryotic photosynthetic proteins. For example, cyanobacterial PSII, CP43/CP47, and PSII OEC peak earlier than their equivalents in photosynthetic eukaryotes, with *Ostreococcus* and other chlorophytes peaking last, and cyanobacterial FtsH and B6F peak earlier than equivalents in photosynthetic eukaryotes.

ssRNA virus 

dsDNA virus 

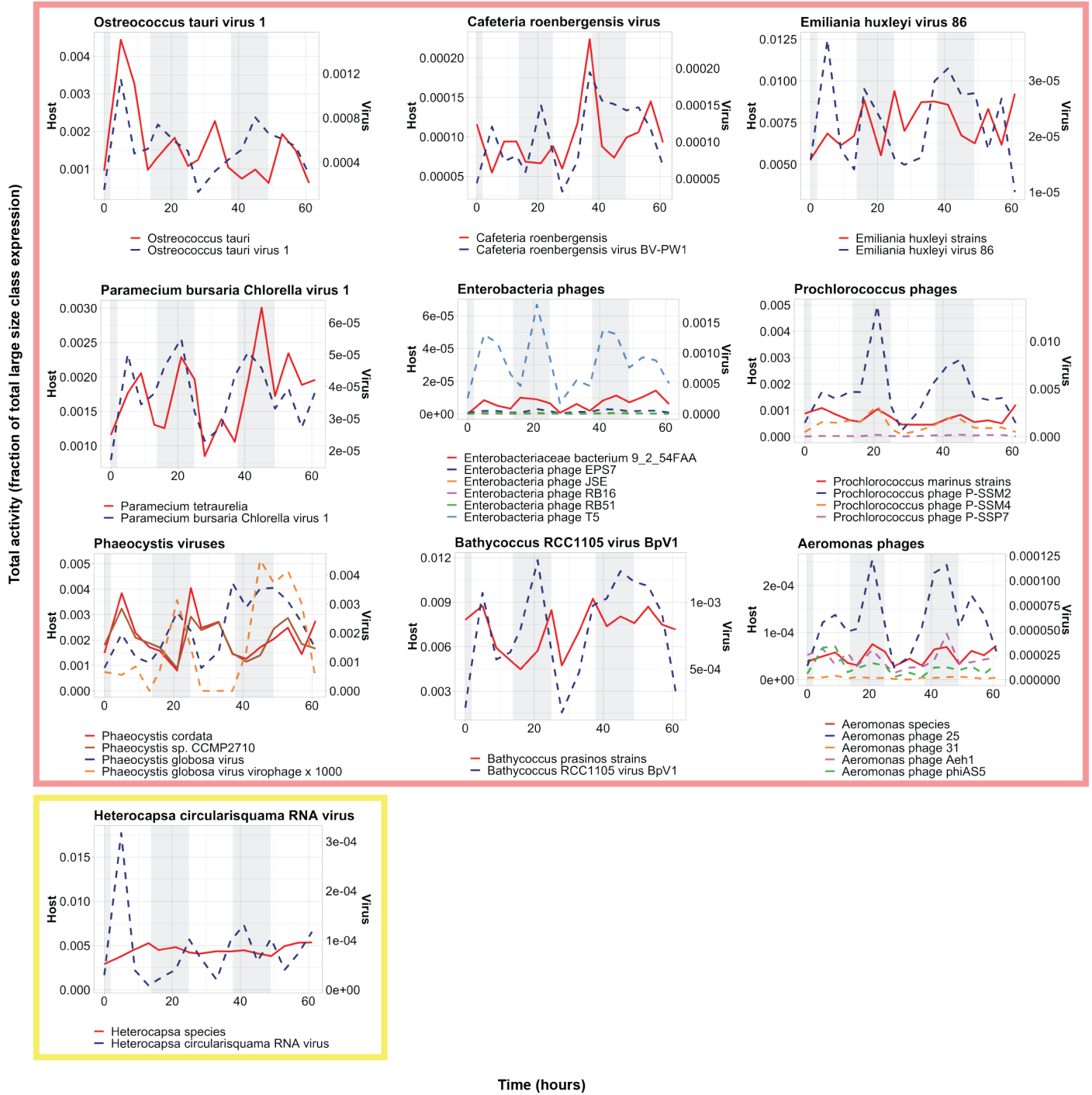


Figure S18 Continuation of Figure 6: virus/host dynamics in the large size class. Viruses and hosts are annotated as the closest reference available in our database, as determined by LPI. Library normalized expression of ORFs classified as ssRNA (yellow) and dsDNA (pink) viruses and their putative hosts by LPI are shown. Putative host expression is represented by solid lines and corresponds to left y-axes; virus expression is represented by dashed lines and corresponds to the right y-axes. *Phaeocystis globulosa* virus virophage expression was multiplied by 10^3 for better visualization. Night hours are shaded in grey.

References

1. Ottesen EA, Young CR, Eppley JM, Ryan JP, Chavez FP, Scholin CA, et al. Pattern and synchrony of gene expression among sympatric marine microbial populations. *Proc Natl Acad Sci*. 2013 Feb 5;110(6):E488–97.
2. Li H, Durbin R. Fast and accurate short read alignment with Burrows-Wheeler transform. *Bioinformatics*. 2009 Jul 15;25(14):1754–60.
3. Bruland KW, Rue EL, Smith GJ. Iron and macronutrients in California coastal upwelling regimes: Implications for diatom blooms. *Limnol Oceanogr*. 2001 Nov;46(7):1661–74.
4. Carradec Q, Pelletier E, Da Silva C, Alberti A, Seeleuthner Y, Blanc-Mathieu R, et al. A global ocean atlas of eukaryotic genes. *Nat Commun*. 2018;9(1).
5. Hutchins DA, DiTullio GR, Zhang Y, Bruland KW. An iron limitation mosaic in the California upwelling regime. *Limnol Oceanogr*. 1998;43(6):1037–54.
6. Johnson KS, Chavez FP, Elrod VA, Fitzwater SE, Pennington JT, Buck KR, et al. The annual cycle of iron and the biological response in Central California coastal waters. *Geophys Res Lett*. 2001;28(7):1247–50.
7. Simmons MP, Sudek S, Monier A, Limardo AJ, Jimenez V, Perle CR, et al. Abundance and biogeography of picoprasinophyte ecotypes and other phytoplankton in the eastern North Pacific Ocean. *Appl Environ Microbiol*. 2016;
8. Siano R, Montresor M, Probert I, Not F, de Vargas C. *Pelagodinium* gen. nov. and *P. béii* comb. nov., a dinoflagellate symbiont of planktonic foraminifera. *Protist*. 2010;161(3):385–99.
9. Töpel M, Pinder MIM, Johansson ON, Kourtchenko O, Godhe A, Clarke AK. Complete genome sequence of *Loktanella vestfoldensis* strain SMR4r, a novel strain isolated from a culture of the chain-forming diatom *Skeletonema marinoi*. *Genome Announc*. 2018;6(12):e01558-17.
10. Bloh AH, Usup G, Ahmad A. *Loktanella* spp. Gb03 as an algicidal bacterium, isolated from the culture of Dinoflagellate *Gambierdiscus belizeanus*. *Vet World*. 2016;9(2):142–6.
11. Pelve EA, Fontanez KM, DeLong EF. Bacterial succession on sinking particles in the ocean's interior. *Front Microbiol*. 2017;8(NOV):2269.
12. Christie JM, Salomon M, Nozue K, Wada M, Briggs WR. LOV (light, oxygen, or voltage) domains of the blue-light photoreceptor phototropin (*nph1*): Binding sites for the chromophore flavin mononucleotide. *Proc Natl Acad Sci*. 1999;96(15):8779–83.
13. Christie JM. Phototropin Blue-Light Receptors. *Annu Rev Plant Biol*. 2007;58(1):21–45.
14. Takahashi F, Yamagata D, Ishikawa M, Fukamatsu Y, Ogura Y, Kasahara M, et al. Aureochrome, a photoreceptor required for photomorphogenesis in stramenopiles. *Proc Natl Acad Sci*. 2007;104(49):19625–30.
15. Glantz ST, Carpenter EJ, Melkonian M, Gardner KH, Boyden ES, Wong GK-S, et al. Functional and topological diversity of LOV domain photoreceptors. *Proc Natl Acad Sci*. 2016;113(11):E1442–51.
16. Ishikawa M, Takahashi F, Nozaki H, Nagasato C, Motomura T, Kataoka H. Distribution and phylogeny of the blue light receptors aureochromes in eukaryotes. *Planta*. 2009;230(3):543–52.
17. Schellenberger Costa B, Sachse M, Jungandreas A, Bartulos CR, Gruber A, Jakob T, et al. Aureochrome 1a Is Involved in the Photoacclimation of the Diatom *Phaeodactylum tricorutum*. *PLoS One*. 2013;8(9).
18. Kianianmomeni A, Hallmann A. Algal photoreceptors: In vivo functions and potential applications. Vol. 239, *Planta*. 2014. p. 1–26.
19. Mateyak MK, Puppek JK, Garino AE, Knapp MC, Colmer SF, Kinzy TG, et al. Demonstration of translation elongation factor 3 activity from a non-fungal species, *Phytophthora infestans*. *PLoS One*. 2018;13(1):1–14.
20. Aylward FO, Eppley JM, Smith JM, Chavez FP, Scholin CA, DeLong EF. Microbial community transcriptional networks are conserved in three domains at ocean basin scales. *Proc Natl Acad Sci*. 2015;112(17):5443–8.

21. Ottesen EA, Young CR, Gifford SM, Eppley JM, Marin R, Schuster SC, et al. Multispecies diel transcriptional oscillations in open ocean heterotrophic bacterial assemblages. *Science* (80-). 2014;345(6193).